Eur. Phys. J. Spec. Top.
https://doi.org/10.1140/epjs/s11734-024-01396-9

THE EUROPEAN PHYSICAL JOURNAL SPECIAL TOPICS

Regular Article

Multimaterial inkjet printing of mechanochromic materials

Muriel Mauron[1], Lucie Castens Vitanov[1], César Michaud[1], Raphaël Wenger[1], Nicolas Muller[1], Roseline Nussbaumer[1], Céline Calvino[2], Christoph Weder[3,4], Stephen Schrettl[3,4,5], Gilbert Gugler[1,a], and Derek John Kiebala[3,4,6,b]

[1] iPrint Institute, HEIA-FR, HES-SO University of Applied Sciences and Arts Western Switzerland, 1700 Fribourg, Switzerland
[2] Cluster of Excellence livMatS, FIT-Freiburg Center for Interactive Materials and Bioinspired Technologies, University of Freiburg, 79110 Freiburg, Germany
[3] Adolphe Merkle Institute, University of Fribourg, 1700 Fribourg, Switzerland
[4] National Competence Center in Research Bio-inspired Materials, University of Fribourg, 1700 Fribourg, Switzerland
[5] TUM School of Life Sciences, Technical University of Munich, 85354 Freising, Germany
[6] Department of Chemistry, Johannes Gutenberg University of Mainz, 55128 Mainz, Germany

Received 30 March 2024 / Accepted 5 November 2024

Abstract Inkjet printing technology achieves the precise deposition of liquid-phase materials via the digitally controlled formation of picoliter-sized droplets. Beyond graphical printing, inkjet printing has been employed for the deposition of separated drops on surfaces or the formation of continuous layers, which allows to construct materials gradients or periodic features that provide enhanced functionalities. Here, we explore the use of multinozzle, drop-on-demand piezoelectric inkjet technology for the manufacturing of mechanochromic materials, i.e., materials that change their color or fluorescence in response to mechanical deformation. To accomplish this, suitable polyurethane polymers of differing hardness grades were tested with a range of organic solvents to formulate low-viscosity, inkjet-printable solutions. Following their rheological characterization, two solutions comprising "soft" and "hard" polyurethanes were selected for in-depth study. The solutions were imbibed with a mechanochromic additive to yield fluorescent inks, which were either dropcast onto polymeric substrates or printed to form checkerboard patterns of alternating hardness using a laboratory-built, multimaterial inkjet platform. Fluorescence imaging and spectroscopy were used to identify different hardness grades in the dropcast and printed materials, as well as to monitor the responses of these gradient materials to mechanical deformation. The insights gained in this study are expected to facilitate the development of inkjet-printable, mechanochromic polymer materials for a wide range of applications.

1 Introduction

Voxelated matter, i.e., materials comprising modular, three-dimensional building blocks, has attracted growing interest due to the fact that such materials can be designed to exhibit tailored surface functionalities and gradient properties [1, 2]. Inkjet-based 3D printing is the method of choice for fabricating voxelated materials with high precision via the digitally controlled formation of picoliter-sized droplets, affording access to a range of material functionalities otherwise inaccessible with conventional processing methods [1]. For example, it has been shown that cell growth and stem cell differentiation can be influenced by printing gradients of biologically active materials [3, 4], and biomedical tomographic data sets have been converted into topographical models via inkjet gradient printing [5]. Beyond biomedical applications, gradients of functional or mechanical characteristics have been demonstrated in 3D-printed metals [6], ceramics [7–9], as well as polymers [10]. This has been achieved by, for example, reactive inkjet printing in which multiple printheads eject pre-polymer reactants onto the same substrate, which form

[a] e-mail: gilbert.gugler@hefr.ch (corresponding author)
[b] e-mail: derek.kiebala@uni-mainz.de (corresponding author)

Published online: 28 November 2024

the desired material in situ with well-resolved microscale features [11]. Moreover, advancements in printhead architecture, optionally assisted by microfluidic mixers, have enabled the printing of materials with gradient properties via a technique known as multimaterial, multinozzle 3D printing, which has greatly expanded the potential for generating new types of inkjet-printed materials [1, 2, 12].

Here, we sought to harness the potential of multimaterial printing to fabricate gradient property materials endowed with mechanochromic functionality, i.e., the ability to change their color or fluorescence in response to mechanical deformation (Fig. 1a). Such mechanochromic materials are particularly useful for reporting stresses and damage in load-bearing materials via an easily detectable and in some cases visually discernible optical signal [13]. The fabrication of such mechanoresponsive polymer materials is made possible by the incorporation of a mechanophore, namely a molecular entity that produces a defined response to external forces via the breakage of a labile bond [14]. Recently, some of us developed a macromolecular additive (tOPV) consisting of two excimer-forming oligo(*p*-phenylene-vinylene) (OPV) dyes connected via a telechelic poly(ethylene-*co*-butylene) backbone (M_n = 3000 g mol/L) that is particularly convenient for conferring mechanochromic behavior to a wide range of polymers [15]. Already when blended in very small quantities (i.e., 0.2–1.0 wt%) into a host polymer, tOPV phase separates from the matrix to form microscopic, fluorescent inclusions whose mechanical and optical properties are closely tied to that of the host matrix, while leaving the mechanical properties of the latter unaffected [16]. This blending process has been used to fabricate films comprising polyurethane (PU), polyisoprene (PI), poly(styrene-*b*-butadiene-*b*-styrene) (SBS) and poly(ε-caprolactone) (PCL) that display strain-dependent changes in fluorescence color [15, 16]. In fact, a change in emission wavelength of a tOPV-containing elastomeric polyurethane was spectroscopically discernible at strains as low as 5% [17], which opens the possibility for sensing applications with unprecedented precision. Taken together, the advantages offered by this mechanochromic additive make it an ideal candidate for exploring the fabrication of mechanochromic materials via inkjet printing.

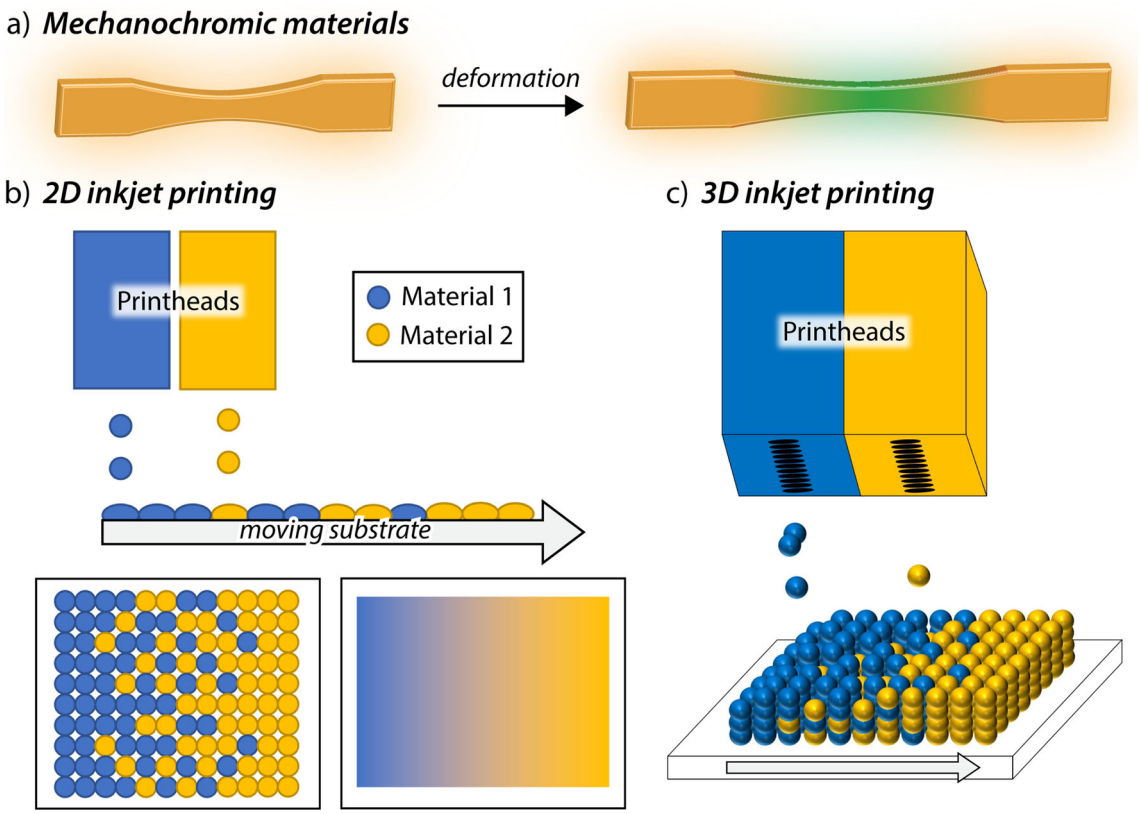

Fig. 1 **a** Operating principle of mechanochromic materials. When subjected to mechanical deformation, the color and/or fluorescence of the material changes from, for example, orange to green. **b**, **c** Overview of how inkjet printing is used to digitally control the composition of a continuous gradient between two materials. **b** Top: side view of a line printed with two printheads each jetting a different polymer-based ink. The ink deposited at each location is digitally controlled by selecting which printhead jets a drop as the substrate passes underneath them. Bottom left: Simplified top-view of a 2D surface printed with two printheads to achieve a gradient. Bottom right: industrial printheads typically feature hundreds to thousands of nozzles, allowing for much smoother gradients. **c** Schematic depicting the deposition of multiple layers on top of each other to create a three-dimensional gradient material

Thus, to pursue the inkjet printing of gradient property, mechanochromic materials, we employed a multimaterial printing system in which two printheads are mounted in parallel and filled with inks containing polymers with two different hardness grades. Droplets of both inks were printed in an alternating fashion on a substrate, enabling the creation of a variable hardness, multilayer material (Fig. 1b, c). Imbibing the polymer inks with the aforementioned mechanochromic additive was possible without the need for additional pre-processing or chemical modification, in contrast to polymer inks formulated with mechanochromic nanoparticles [18] or microgels [19]. This yielded patterned fluorescent films, which allowed us to investigate the mixing dynamics of the different materials at the voxel–voxel interface using fluorescence imaging and spectroscopy. Finally, we show that mechanical deformation of the substrate-supported, gradient-hardness films changes their fluorescence in a quantifiable fashion, constituting an important step toward the realization of inkjet-printed, mechanochromic multimaterials.

2 Materials and methods

2.1 Ink formulation

As the basis for the mechanochromic polymer inks formulated in this study, commercially available polyurethanes (PUs) of different hardness, namely "soft" PU (PU-S, shore hardness 35A) and "hard" PU (PU-H, shore hardness 80A) were provided by BASF and Huntsmann, respectively. 1,4-Dioxane solvent (also referred to as dioxane; 99%+ purity) was purchased from Acros Organics. The solvents 1-methyl-2-pyrrolidinone (NMP; 99%) and 2-butoxyethyl acetate (BCA; 99%) were purchased from Sigma-Aldrich. The telechelic oligo (*p*-phenylene-vinylene) (tOPV) mechanochromic additive used in the final ink formulations was prepared as previously reported, omitting the final purification step [15]. Hence, a greater amount of tOPV was used for the ink formulations (i.e., 5 wt% vs. polymer) in comparison to previous studies (i.e., 0.2–1 wt% vs. polymer) to ensure sufficient assembly of difunctional tOPV in the printed samples. Polymer solutions were made by adding either PU-S or PU-H to dioxane in a glass vial, which was placed on a shaker at 100 rpm for at least 12 h to ensure complete dissolution. All dioxane-based ink solutions were prepared in a well-ventilated fume hood to avoid inhalation of dioxane vapors, which have been shown in animal studies to exhibit carcinogenicity [20, 21].

Chemical compatibility tests were performed between the candidate solvents and the printheads following the manufacturer's instructions. To carry out these tests, nine different parts of the printhead were weighed, immersed individually in 30 mL of the solvent being tested in amber glass bottles, and placed in an oven at 60 °C for 6 weeks. At 2-week intervals, the parts were cleaned by immersion first in *n*-butyl lactate (99%, ThermoScientific) and then in propan-2-ol (99%, Thommen-Furler AG). After evaporation of the cleaning solvents, the parts were re-weighed and again immersed in the test solvent at 60 °C. The data was sent back to the manufacturer, who analyzed the changes in weight of each piece to assess compatibility between the solvent and the printhead.

The rheological properties of the polymer solutions were analyzed with a Piezo Axial Vibrator (Tri-PAV) rheometer from TriJet at room temperature from 100 Hz to 10 kHz to identify suitable solvents and polymer concentrations for inkjet printing [22]. The surface energy, contact angle and surface tension of the solutions were measured with the OCA25 contact angle and drop shape measuring device from Dataphysics. The surface energy of the substrate was calculated using the contact angles of droplets ($V \approx 2$ μL) of water, ethylene glycol, and diiodomethane, the Young Laplace equation, and the Owens–Wendt–Rabel and Kaelble (OWRK) model. The static surface tension for droplets ($V = 12$–15 μL) of each ink was measured with the same device using the pendant drop method.

2.2 Inkjet printing

To enable simultaneous printing of multiple different PU inks, an inkjet printing platform was built that incorporates two Seiko RC1536L printheads, an ink distribution system, and a stage movable along the *x*-, *y*-, and *z*-axes, all of which were governed by a Beckhoff Programmable Logic Controller (PLC) (Fig. S1). The Seiko RC1536L printheads, which feature four rows of 384 nozzles (totaling 1536 available nozzles with a maximum resolution of 360 dpi), were selected for their generally good chemical compatibility and suitability for printing at relatively high viscosity (i.e., up to 20 mPa s). The platform is capable of simultaneously printing materials in 2D with up to three printheads, as well as 3D materials by sequentially printing multiple 2D layers as depicted in Fig. 1c. The volume and speed of ink droplets exiting the printhead nozzles during the printing process were determined by acquiring images of the droplets in flight using a camera (33GP031 from The Imaging Source) with a 0.7–4.5X zoom lens (Model HY-180XA from Hayear), combined with a strobing light source and a homemade triggering system. A bespoke Matlab script was used for synchronizing the operations and extracting key features from the images, such as the drop speed, volume, and shape. The printheads and their waveforms were controlled with driving electronics from Aewa and their dedicated APRINT software. Selected inks containing the mechanochromic additive were deposited by dropcasting or inkjet printing at room temperature on a PU substrate fixed on a heating plate at

40 °C, followed by drying at 60 °C for 12 h. Round substrates (55 mm diameter, 0.3 mm thickness) were produced by Torson Injex by injection molding of Elastollan E565A12P (BASF), and rectangular substrates with dimensions of 60 × 20 × 0.38 mm (length × width × thickness) of the same material were produced by injection molding at the iRap Institute of the HEIA in Fribourg. During operation, the inkjet printer was enclosed and an extraction arm was used to remove aerosols and potentially toxic dioxane vapors produced during printing (Fig. S1b).

2.3 Fluorescence spectroscopy and microscopy

Fluorescence changes in printed PU/tOPV films were measured spectroscopically as a function of mechanical stress using an Ocean Optics USB 4000 spectrometer connected to an Ocean Optics LS-450 LED light source with an excitation wavelength of $\lambda_{ex} = 380$ nm and an Ocean Optics QR230-7-XSR SMA 905 optical fiber. The extent of aggregation of the excimer-forming end groups of the tOPV macromolecule, which is influenced by processing conditions, changes in temperature, and the application of mechanical force, were probed by measuring fluorescence spectra and determining the monomer-to-excimer emission intensity ratio (I_{510}/I_{630}). Mechanical deformation of tOPV-containing materials has been shown to reliably result in an increase in I_{510}/I_{630}, which occurs when the distance between adjacent tOPV emitters is increased [16, 17]. The value was calculated from the solid-state fluorescence spectra by taking the intensity value at the maximum of the monomer emission peak ($\lambda_{max} = 510$ nm) divided by the maximum of the excimer emission peak ($\lambda_{max} = 630$ nm). Samples were placed on top of a piece of black paper, and the optical fiber was oriented normal to the surface at a distance of 2 mm, resulting in a spot size of approximately 800 μm from which the diffuse reflectance was measured. Spectra were recorded before, after, or during application of mechanical stress and fluorescence data were acquired using Stream Basic software. Stress–strain data collected during these measurements was recorded by uniaxial deformation of rectangular samples with dimensions of 30 × 3 × 0.3–0.4 mm (length × width × thickness) at 100% min^{-1} using a Linkam TST350 microtensile stage equipped with a 20 N load cell and controlled by the accompanying Linksys32 software. A pre-load force of 0.1 N was applied before initiating deformation.

Confocal microscopy images were acquired on a Zeiss LSM 710 Meta confocal laser scanning microscope (CLSM) equipped with an Ar laser (max. power 25 mW) and a spectrometer allowing acquisition of emitted light in two channels at nanometer precision within the visible range. All data was recorded using a 63X/1.3NA oil lens at a lateral resolution of 132 nm. Channel 1 recorded emission between 461 and 525 nm (i.e., primarily tOPV monomer emission), and channel 2 recorded emission between 550 and 725 nm (i.e., primarily tOPV excimer emission). Both channels used a laser excitation of 458 nm. For a given region of interest (ROI) at the surface of the sample, the monomer-to-excimer ratio (for CLSM images denoted as I_M/I_E) was obtained by dividing the mean pixel intensity for the ROI in channel 1 by the mean intensity for the ROI in channel 2. While I_M/I_E values obtained by CLSM image analysis are not directly comparable to the I_{510}/I_{630} values obtained by solid-state fluorescence spectroscopy, the trends in these values (e.g., for PU of different hardness, or when subjecting the films to mechanical force) mirror each other. CLSM images were acquired as 16-bit grayscale images, and false colors of green and orange were applied to the monomer and excimer channels, respectively, to match the visible fluorescence colors of the corresponding assembly states of tOPV. Thus, combined-channel CLSM images have a yellow-green appearance after false coloring.

Printed PU/tOPV layers on Elastollan substrates were imaged by cutting a 0.5 × 0.5 cm square piece and placing it on a glass slide. Two drops of halogen-free, non-fluorescent Cargille Immersion Oil Type HF (i.e., refractive index-matching oil) were added to the sample, onto which a glass cover slip of approximately 0.17 mm thickness was placed. One drop of the same immersion oil was then placed on the lens of the confocal microscope, after which the glass slide and sample assembly was inverted such that the cover slip was facing downwards and placed on the microscope stage. The lens was then raised so that the oil came into contact with the glass cover slip, creating an air-free path for the excitation laser of the laser confocal scanning microscope to pass through the sample. Equibiaxial stretching was carried out on samples using a custom-built stretching device that applied radial strain in all directions (see Ref. [16] for a detailed description of the setup).

3 Results and discussion

3.1 Polymer solution testing

As a first step in the formulation of printable mechanochromic inks, solubility tests were carried out with the PU polymers and the tOPV mechanochromic additive in a range of organic solvents with varying hydrophobicity and boiling points. Of the solvents tested, tOPV showed the best solubility at 1 mg/mL in dioxane, tetrahydrofuran (THF), *N*-methyl-2-pyrrolidinone (NMP), and mixtures of NMP and 2-butoxyethyl acetate (BCA) with at least 25 wt% of NMP. tOPV remained well dissolved in these solutions at room temperature over the course of 24 h as

indicated by the solutions' green fluorescent color, thus serving as a good indicator that no tOPV would precipitate inside the printhead during the printing process. The other solvents tested that did not fully dissolve the PU (in the range of 15–20 mg/mL) or tOPV (at 1 mg/mL) include: *n*-hexane, xylene, isophorone, BCA (99%), methyl ethyl ketone, ethyl acetate, methanol, ethanol, propanol, 1,5-pentanediol, glycerol, ethylene glycol, propylene glycol, 2-methoxyethanol, and triethanolamine.

After subjecting the different components of the Seiko RC1536L printhead used in the lab-built inkjet printer to chemical compatibility tests (see Sect. 2.1 for details), the results showed dioxane and NMP/BCA 25/75 wt% to be the most promising solvent candidates (Table S1). Polymer solutions were then made by dissolving pellets of PU-S and PU-H in dioxane and NMP/BCA 25/75 wt% at 20 mg/mL, which was the concentration used for all further tests. To assess the printability of the different ink formulations, rheological measurements were carried out on solutions of PU-S and PU-H without the tOPV additive, given that the small amounts of tOPV to be added in the final inks would not affect the rheological properties of the latter. The results showed that all four polymer solutions exhibit complex viscosities ranging from 3.5 to 8 mPa s between 20 and 3000 Hz applied frequency (Fig. 2a), well within the range of 2–20 mPa s recommended for industrial printheads [23, 24]. Moreover, the elasticity of the solutions, defined as the ratio of the storage modulus G' to the absolute value of the complex modulus —G*—, was found to be sufficiently low, i.e., near zero for the dioxane-based solutions and less than 0.1 for NMP/BCA 25/75 wt% up to 3 kHz (Fig. 2b), indicating that they could be reliably jetted through the printhead nozzle. Thus, dioxane was selected as the preferred solvent to formulate the mechanochromic inks based on the lower elasticity of the dioxane-based PU solutions. Finally, printhead waveform optimization was performed by acquiring and analyzing real-time images of polymer solution droplets ejected from the printhead nozzles (Fig. 3) and iterating over the waveform parameters until suitable drop characteristics were achieved. The waveforms of

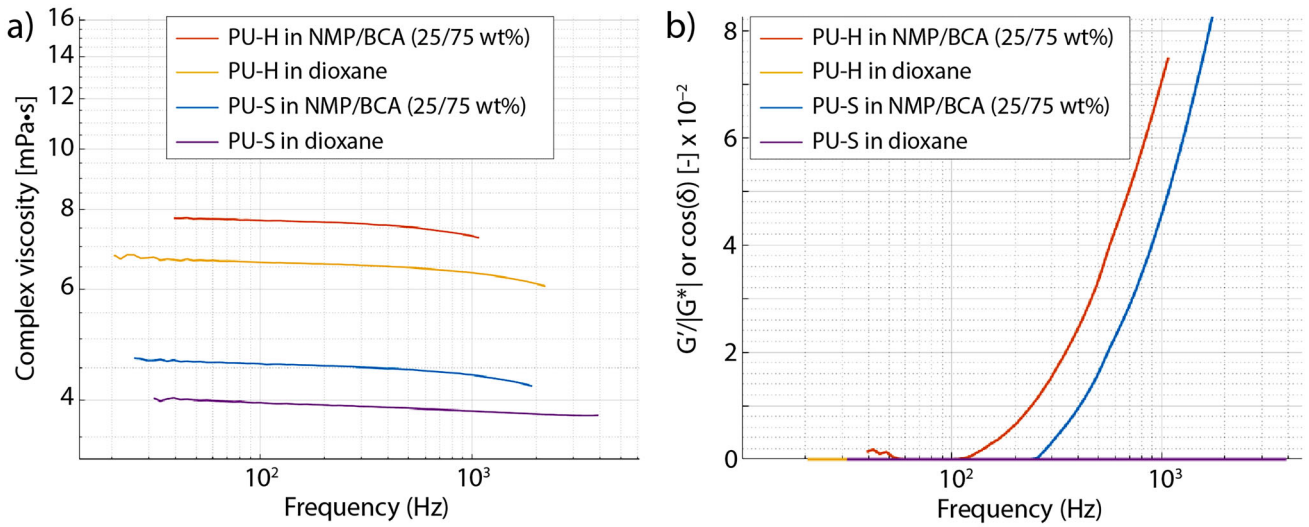

Fig. 2 Rheological measurements carried out on PU-S and PU-H at 20 mg/mL in both dioxane and NMP/BCA 25/75 wt% solvents. Both **a** complex viscosity and **b** elasticity (G'/—G*—) were measured as a function of applied frequency at 25 °C

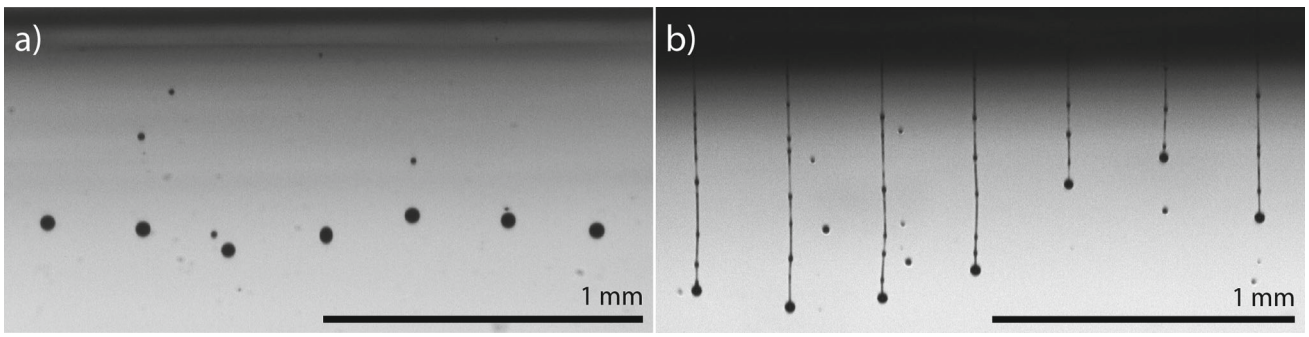

Fig. 3 Real-time images of polymer solution droplets ejected from seven adjacent nozzles in one row of the printhead at **a** 20 V ($v_{\mathrm{drop}} \approx 5$ m/s) and at **b** 28 V ($v_{\mathrm{drop}} \approx 8$ m/s). Scale bars = 1 mm

the Seiko RC1536L printheads were initially optimized to achieve a minimum drop speed of 5 m/s and a drop size of 25 pL with the selected solutions. However, the quick drying of the solution in the nozzles prevented stable printing. Thus, a higher waveform voltage was employed (i.e., ca. 28V instead of the 20 V initially used) to produce faster-traveling droplets ($v_{\mathrm{drop}} \approx 8$ m/s) that avoided precipitation of the polymer in the printhead during printing.

3.2 Film–substrate interactions

Next, we investigated the interaction of the dioxane polymer solutions with an Elastollan polymer film (thickness = 1 mm), which was to be used as the substrate for dropcasting and ultimately printing the inks. To this end, we deposited a 10 µL drop of each solution onto the substrate and measured the surface tension of the solution droplet, the solution–substrate contact angle, and the surface energy of the substrate. The dioxane-based polymer solutions were found to exhibit a low static surface tension typical of solvent-based inks, namely 33.2 and 25.6 mN/m for PU-S and PU-H in dioxane, respectively, both of which fall below the 40 mN/m limit for inkjet drop ejection [25]. The surface energy of the substrate was found to be 47.6 mN/m, which exceeds the surface tension and indicates excellent wettability. Finally, the contact angles were determined to be 21.8° ± 0.9° and 23.3° ± 2° for PU-S and PU-H in dioxane, respectively, further confirming that these inks wet the substrate well.

3.3 Mechanochromism of dropcast films

To endow these printable polymer solutions with mechanochromic properties, the tOPV additive was dissolved in each solution at a concentration of 1 mg/mL to produce the final ink formulations (**Ink A**: PU-S [20 mg/mL] + tOPV [1 mg/mL] in dioxane, and **Ink B**: PU-H [20 mg/mL] + tOPV [1 mg/mL] in dioxane). The inks were dropcast onto Elastollan substrates and subsequently dried at 60 °C for 12 h in vacuo to yield thin films that exhibited a homogeneous yellow fluorescent color under UV illumination, indicating proper assembly of the tOPV additive within the films [15, 17]. The two inks were dropcast next to each other on the substrate in such a way that produced a "mixed region" or interface where the two inks overlapped (Fig. 4a). The mechanical properties of the substrate were largely unaffected by the dropcast inks, with the exception of a slight increase in mechanical stress during strain hardening (Fig. S2).

Solid-state fluorescence spectroscopy measurements revealed that, in the as-prepared films, the monomer-to-excimer ratio of "soft" ink A ($I_{510}/I_{630} = 1.02$) was lower than that of "hard" ink B ($I_{510}/I_{630} = 1.18$), and that of the mixed region ($I_{510}/I_{630} = 1.13$) was in between the two. Next, the substrate was subjected to uniaxial tensile deformation at a strain rate of 100% min^{-1} up to 250% strain (the resulting stress–strain curve is shown in the

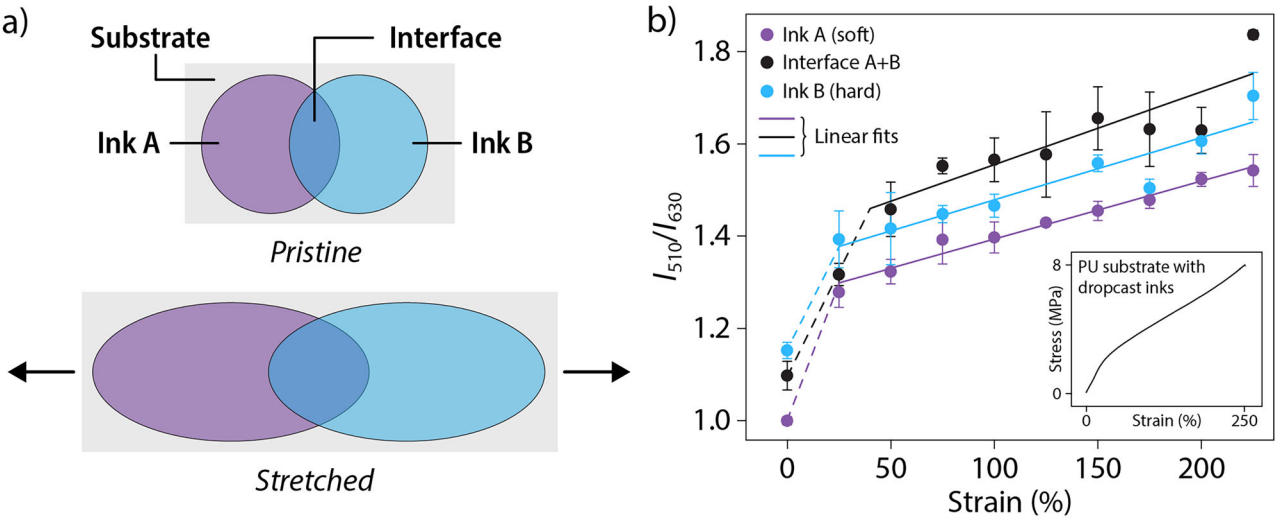

Fig. 4 **a** Schematic depicting films made by dropcasting inks A and B onto the Elastollan substrate. Upper panel: regions of pure ink A and ink B are indicated, as well as the mixed region or interface where the two inks overlap. Lower panel: uniaxial stretching of the substrate caused the dropcast films to deform along the stretching axis. **b** Plot of the monomer-to-excimer fluorescence intensity ratio (I_{510}/I_{630}) of regions of pure ink A, pure ink B, and the interface where the two regions mix, as a function of applied strain. Datapoints represent the average of three fluorescence measurements within each region, and error bars represent one standard deviation. Dashed lines serve as a guide to the eye; solid lines represent linear fits performed between 25 and 225% strain for inks A and B, and between 50 and 225% strain for the mixed region. Inset: stress–strain curve of the Elastollan substrate with the dropcast films measured during the test

inset in Fig. 4b), and the I_{510}/I_{630} for each region of the dropcast film was monitored. Notably, the I_{510}/I_{630} for all regions (i.e., pure inks A and B, as well as the mixed region) increased sharply between 0 and 50% strain, after which the I_{510}/I_{630} of each region continued to increase in a linear fashion until the end of the test (Fig. 4b). This linear fluorescence response to uniaxial deformation closely mirrors that of previously reported PU/tOPV blend films that feature different slopes for low- vs. high-strain deformation [17], thus confirming that force is transferred between the substrate and dropcast films. Notably, a greater initial increase in I_{510}/I_{630}, as well as a slightly steeper slope at high strains, is observed for the interfacial region, suggesting that microscale domain boundaries between partially demixed PU-S and PU-H exert more local strain on the tOPV additive when deformed. The mechanochromic response displayed by the dropcast films was found to be consistent across multiple samples, as well as reversible over at least three cycles (Fig. S3). Taken together, these results confirm that the PU/tOPV inks formulated herein can be readily used to fabricate substrate-supported, mechanochromic films.

After confirming the mechanochromism of dropcast films made from polymer inks A and B, we turned to confocal laser scanning microscopy (CLSM) to more closely study the morphology of the films, particularly at the mixing interface. To this end, CLSM images were acquired. The monomer and excimer emission of the dropcast films were recorded in two separate channels, thus allowing for the determination of the monomer-to-excimer emission ratio (denoted as I_M/I_E for CLSM images) with micrometer-resolution for different areas of the film via image analysis (see Sect. 2.3 for details). Distinct areas comprising inks A and B were readily identifiable by their fluorescence; namely, the area formed by "soft" ink A consistently exhibited a lower I_M/I_E than regions formed by "hard" ink B (Fig. 5). In some regions, a quasi-linear decrease in I_M/I_E is observed across the mixing zone when moving

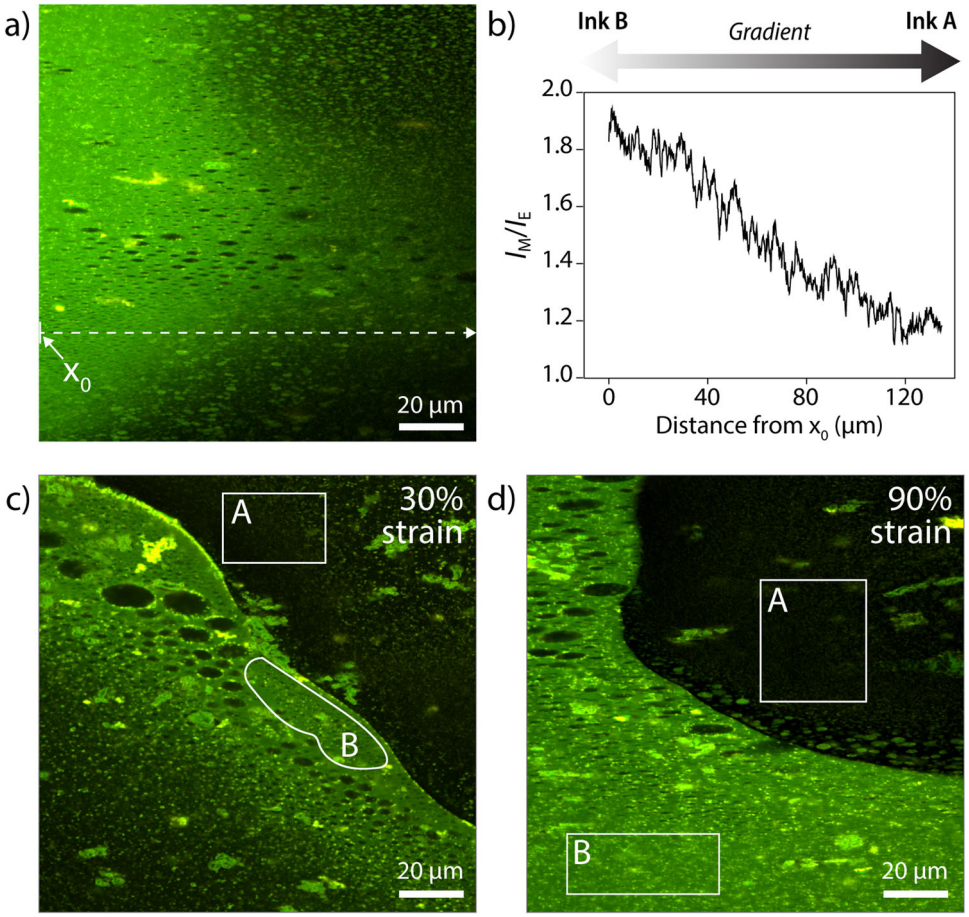

Fig. 5 **a** Combined-channel 2D CLSM image of an interfacial region between inks A and B on the same film. **b** I_M/I_E values determined as a function of x-position moving left to right along the dashed line in **a**. **c**, **d** Confocal microscopy images of the mixing interface of inks A and B, which were dropcast onto an Elastollan substrate and subjected to equibiaxial strains of **c** 30% and **d** 90%. Images were recorded in two channels, i.e., the monomer (Ch 1: λ_{em} = 461–525 nm) and excimer (Ch 2: λ_{em} = 550–725 nm) emission channels and then merged to obtain the combined-channel images shown. At each strain, the monomer-to-excimer emission ratio (I_M/I_E) was determined for the indicated regions of interest for inks A and B (labeled as A and B, respectively) by dividing the mean pixel intensity of channel 1 by that of channel 2. Scale bars = 20 μm

from ink B (left side of the image in Fig. 5a) to ink A (right side), indicative of a compositional gradient between the two inks (Fig. 5a, b). On the other hand, some areas of the mixing zone exhibit a sharp transition between the two inks (Fig. 5c, d, Fig. S4), likely stemming from limited miscibility of the two polymers and selective dewetting processes that occurred during drying. Moreover, low-I_M/I_E features were observed interspersed in regions of ink B and vice versa, pointing to a complex mixing behavior between the two inks (Fig. 5a, c, d).

Next, the dropcast films were subjected to equibiaxial strain (i.e., radial strain applied equally in all directions) using a custom-built stretching device (see Ref. [16] for details) and imaged via CLSM. At each strain, parts of film comprising either ink A or B were identified, and the I_M/I_E was determined for the indicated regions by dividing the mean pixel intensity of the monomer channel by that of the excimer channel. The results show that, when increasing the equibiaxial strain from 30 to 90%, the I_M/I_E for ink A increases from 0.98 to 1.09, and the I_M/I_E for ink B increases from 1.47 to 1.57 (Fig. 5c, d). These observations are in agreement with the increase in I_{510}/I_{630} measured for both inks A and B via solid-state fluorescence spectroscopy (Fig. 4b) and further corroborate that PU/tOPV films formed from the dioxane-based inks formulated herein exhibit mechanochromism.

3.4 Inkjet printing trials

Finally, we sought to employ our inkjet printing setup to fabricate mechanochromic films with gradient mechanical properties. As a first test, polymer solutions A and B (i.e., inks A and B without the tOPV additive) were printed in an alternating fashion onto a circular Elastollan substrate to create a checkerboard pattern (Fig. 6a, b). Multiple passes were made by the printhead to deposit a total of 20 layers, which yielded a printed film less than 1 µm thick with a feature resolution of 2 mm in the x,y-plane as seen by the naked eye. While printing trials with dioxane alone revealed partial dissolution of the surface of the substrate (Fig. S5), such effects are expected to be less pronounced when printing multi-layer patterns with the mechanochromic inks, given that the PU deposited from previously printed layers blocks direct contact between dioxane and the substrate. Indeed, the mechanical properties of the substrate were not affected by the printing of 20 layers of the mechanochromic ink (Fig. S6), indicating that damage to the substrate as a consequence of the printing process is negligible. The same process was then carried out with tOPV-containing inks A and B, and the 20-layer printed pattern was imaged by CLSM (Fig. 6c). While the interface between the "soft" ink A and "hard" ink B is clearly discernible, many satellite droplets of the hard PU are visible at least 0.5 mm into the soft PU region. This is largely a consequence of the fact that, in order to avoid the inks drying in the printhead during deposition, a higher waveform voltage was used to increase the speed of the droplet ejection. Thus, the CLSM images of the additive-containing, printed PU patterns reveal that the high voltage and speed of the printing process diminish the accuracy and therefore resolution of the printed features. Moreover, many non-fluorescent areas are visible within the hard PU region, indicating that this PU shows a greater tendency to dewet from the substrate during printing and leave some

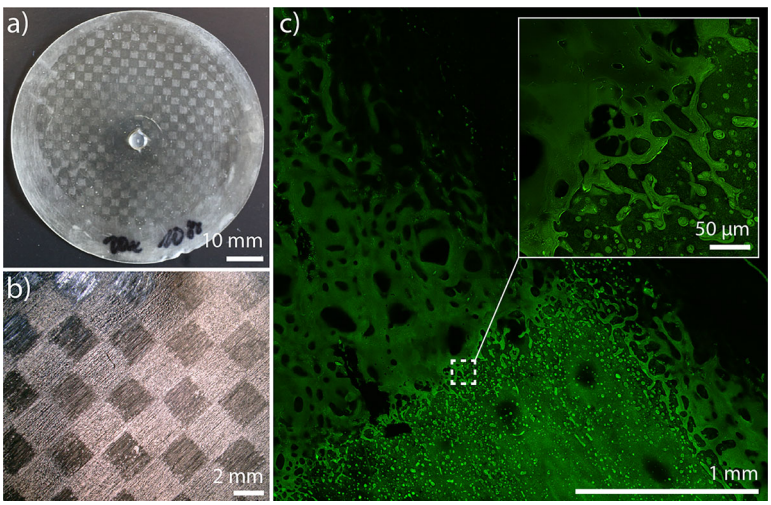

Fig. 6 **a** Image of a checkerboard pattern created by printing polymer solutions of "soft" PU-S and "hard" PU-H (c(dioxane) = 20 mg/mL) in an alternating fashion on a circular Elastollan substrate. Multiple passes were made by the printhead to deposit a total of 20 layers. Scale bar = 10 mm. **b** Magnified view of a portion of the sample shown in **a**. Scale bar = 2 mm. **c** Combined-channel CLSM image of the intersection of two of the checkerboard squares comprising "soft" ink A (lower right region) and "hard" ink A (upper left region) that had been printed on the same type of circular Elastollan substrate as shown in **a**. Scale bar = 1 mm. Inset: Magnified CLSM image of the indicated interfacial region between the two inks (scale bar = 50 µm)

portions of the substrate uncovered. To overcome these obstacles, further trials are needed to identify alternative polymer materials that are compatible with inkjet-printable solvents and that, like films printed from ink B, do not show evidence of dewetting from the substrate when multiple-pass printing is performed. Moreover, the use of a less volatile solvent could allow for slower printing, which may avoid the generation of satellite droplets that breach the hard-soft polymer interface.

4 Conclusion

In the present work, the printing of gradient-property, patterned polymer films with mechanochromic sensing capability was investigated. In order to realize the fabrication of such films, a multimaterial inkjet printing platform was developed that allows for the simultaneous printing of two different polymer solutions into multilayer voxels of alternating composition. After extensive testing was carried out on candidate polymers solutions to evaluate their printability, "hard" and "soft" PU solutions in dioxane were selected for their desirable rheological properties and compatibility with the printheads. A mechanochromic additive was mixed into the solutions to obtain fluorescent polymer inks, which were either dropcast or printed in different patterns onto a stretchable polymer substrate. The different inks were readily identifiable via their distinct fluorescence, and an in-depth evaluation of the microscale features of the fluorescent films shed light on complex mixing behaviors at the interface between the two inks. Importantly, when subjected to mechanical deformation, both dropcast and inkjet-printed, multimaterial films exhibited mechanochromic behavior that could be tracked individually for each voxel. The insights gained into the properties of inkjet-printable polymer inks and the microscale characterization of patterned polymers are expected to greatly facilitate the development of tailor-made functional materials with complex property profiles otherwise inaccessible by conventional processing techniques.

Supplementary Information The online version contains supplementary material available at https://doi.org/10.1140/epjs/s11734-024-01396-9.

Acknowledgements M.M., L.C.V., C.M., R.W., R.N., N.M., and G.G. acknowledge financial support through funding from HES-SO University of Applied Sciences and Arts Western Switzerland, Engineering and Architecture, Grant Smart-MatJet 114624. C.W., S.S., and D.J.K. gratefully acknowledge financial support through the National Center of Competence in Research (NCCR) (Grant no. 51NF40-182881) Bio-inspired Materials, a research instrument of the Swiss National Science Foundation (SNF), and funding from the Adolphe Merkle Foundation.

Author contribution statement

MM, LCV, CM, and RW built the inkjet printing device; carried out the printhead compatibility testing, polymer solution characterization, and substrate analysis; optimized the dropcasting protocol; and carried out the inkjet printing trials. DJK carried out solubility testing and prepared the mechanochromic inks, measured the fluorescence of dropcast films during tensile testing, and acquired and analyzed the confocal microscopy images of printed films. CC synthesized the mechanochromic additive. SS and GG designed the original concept for the study and provided guidance throughout the project. DJK, MM, RN, RW, and NM wrote the manuscript, which was edited by CW. All authors have given approval to the final version of the manuscript.

Funding Open access funding provided by University of Fribourg.

Data availability The datasets generated and analyzed during the current study are available from the corresponding author on reasonable request.

Declarations

Conflict of interest The authors declare no competing financial interests.

References

1. M.A. Skylar-Scott, J. Mueller, C.W. Visser, J.A. Lewis, Voxelated soft matter via multimaterial multinozzle 3D printing. Nature **575**(7782), 330–335 (2019). https://doi.org/10.1038/s41586-019-1736-8
2. E.L. Doubrovski, E.Y. Tsai, D. Dikovsky, J.M.P. Geraedts, H. Herr, N. Oxman, Voxel-based fabrication through material property mapping: a design method for bitmap printing. Comput. Aided Des. **60**, 3–13 (2015). https://doi.org/10.1016/j.cad.2014.05.010
3. S. Ilkhanizadeh, A. Teixeira, O. Hermanson, Inkjet printing of macromolecules on hydrogels to steer neural stem cell differentiation. Biomaterials **28**(27), 3936–3943 (2007). https://doi.org/10.1016/j.biomaterials.2007.05.018
4. K. Cai, H. Dong, C. Chen, L. Yang, K.D. Jandt, L. Deng, Inkjet printing of laminin gradient to investigate endothelial cellular alignment. Colloids Surf. B Biointerfaces **72**(2), 230–235 (2009). https://doi.org/10.1016/j.colsurfb.2009.04.008
5. A. Hosny, S.J. Keating, J.D. Dilley, B. Ripley, T. Kelil, S. Pieper, D. Kolb, C. Bader, A.-M. Pobloth, M. Griffin, R. Nezafat, G. Duda, E.A. Chiocca, J.R. Stone, J.S. Michaelson, M.N. Dean, N. Oxman, J.C. Weaver, From improved diagnostics to presurgical planning: high-resolution functionally graded multimaterial 3D printing of biomedical tomographic data sets. 3D Print. Addit. Manuf. **5**(2), 103–113 (2018). https://doi.org/10.1089/3dp.2017.0140
6. D. Godlinski, S. Morvan, Steel parts with tailored material gradients by 3D-printing using nano-particulate Ink, in *Materials Science Forum* vol. 492–493 (Trans Tech Publications Ltd., Stafa, 2005), p. 679–684. https://doi.org/10.4028/0-87849-970-9.679
7. M. Mott, J.R.G. Evans, Zirconia/alumina functionally graded material made by ceramic ink jet printing. Mater. Sci. Eng. A **271**(1–2), 344–352 (1999). https://doi.org/10.1016/S0921-5093(99)00266-X
8. M.A.F. Afzal, P. Kesarwani, K.M. Reddy, S. Kalmodia, B. Basu, K. Balani, Functionally graded hydroxyapatite-alumina-zirconia biocomposite: synergy of toughness and biocompatibility. Mater. Sci. Eng. C **32**(5), 1164–1173 (2012). https://doi.org/10.1016/j.msec.2012.03.003
9. J.-H. Lee, J.-H. Kim, K.-T. Hwang, H.-J. Hwang, K.-S. Han, Digital inkjet printing in three dimensions with multiple ceramic compositions. J. Eur. Ceram. Soc. **41**(2), 1490–1497 (2021). https://doi.org/10.1016/j.jeurceramsoc.2020.09.044
10. M. Schaffner, J.A. Faber, L. Pianegonda, P.A. Rühs, F. Coulter, A.R. Studart, 3D printing of robotic soft actuators with programmable bioinspired architectures. Nat. Commun. **9**(1), 878 (2018). https://doi.org/10.1038/s41467-018-03216-w
11. F. Schuster, T. Hirth, A. Weber, Reactive inkjet printing of polyethylene glycol and isocyanate based inks to create porous polyurethane structures. J. Appl. Polym. Sci. **136**(3), 46977 (2019). https://doi.org/10.1002/app.46977
12. J.O. Hardin, T.J. Ober, A.D. Valentine, J.A. Lewis, Microfluidic printheads for multimaterial 3D printing of viscoelastic inks. Adv. Mater. **27**(21), 3279–3284 (2015). https://doi.org/10.1002/adma.201500222
13. H. Traeger, D.J. Kiebala, C. Weder, S. Schrettl, From molecules to polymers-harnessing inter- and intramolecular interactions to create mechanochromic materials. Macromol. Rapid Commun. **42**(1), 2000573 (2021). https://doi.org/10.1002/marc.202000573
14. N. Deneke, M.L. Rencheck, C.S. Davis, An engineer's introduction to mechanophores. Soft Matter **16**(27), 6230–6252 (2020). https://doi.org/10.1039/D0SM00465K
15. C. Calvino, Y. Sagara, V. Buclin, A.P. Haehnel, A. Prado, C. Aeby, Y.C. Simon, S. Schrettl, C. Weder, Mechanoresponsive, luminescent polymer blends based on an excimer-forming telechelic macromolecule. Macromol. Rapid Commun. **40**(1), 1800705 (2019). https://doi.org/10.1002/marc.201800705
16. D.J. Kiebala, R. Style, D. Vanhecke, C. Calvino, C. Weder, S. Schrettl, Sub-micrometer mechanochromic inclusions enable strain sensing in polymers. Adv. Funct. Mater. **33**(50), 2304938 (2023). https://doi.org/10.1002/adfm.202304938
17. D.J. Kiebala, Z. Fan, C. Calvino, L. Fehlmann, S. Schrettl, C. Weder, Mechanoresponsive elastomers made with excimer-forming telechelics. Org. Mater. **2**(4), 313–322 (2020). https://doi.org/10.1055/s-0040-1721052
18. K. Ogumi, K. Nagata, Y. Takimoto, K. Mishiba, Y. Matsuo, Inkjet printing of mechanochromic fluorenylidene-acridane. Sci. Rep. **12**(1), 16997 (2022). https://doi.org/10.1038/s41598-022-21600-x
19. B. Xu, H. Wang, Z. Luo, J. Yang, Z. Wang, Multi-material 3D printing of mechanochromic double network hydrogels for on-demand patterning. ACS Appl. Mater. Interfaces **15**(8), 11122–11130 (2023). https://doi.org/10.1021/acsami.2c22564
20. T. Kasai, M. Saito, H. Senoh, Y. Umeda, S. Aiso, H. Ohbayashi, T. Nishizawa, K. Nagano, S. Fukushima, Thirteen-week inhalation toxicity of 1,4-dioxane in rats. Inhalation Toxicol. **20**(10), 961–971 (2008). https://doi.org/10.1080/08958370802105397
21. U.S. EPA, Toxicological review of 1,4-dioxane (with inhalation update) (CAS no. 123–91-1) in support of summary information on the integrated risk information system (IRIS). EPA Report, U.S. Environmental Protection Agency, Washington, D.C., U.S. (2013)
22. Z. Hussain, Z. Kiaee, M. Nazarzadeh, C. Reichel, S. Tepner, T. Tuladhar, M. Jahn, R. Keding, High-frequency rheological and piezo-voltage waveform characterization of inkjet-printed polymer-based dopant-source inks. Micromachines **14**(1), 80 (2022). https://doi.org/10.3390/mi14010080
23. W. Zapka (ed.), *Handbook of Industrial Inkjet Printing: A Full System Approach*, 1st edn. (Wiley, New York, 2017). https://doi.org/10.1002/9783527687169

24. T. Tuladhar, Measurement of complex rheology and jettability of inkjet inks, in *Inkjet Printing in Industry*, 1st edn., ed. by W. Zapka (Wiley, New YorK, 2022), pp.655–693. https://doi.org/10.1002/9783527828074.ch28
25. B. He, S. Yang, Z. Qin, B. Wen, C. Zhang, The roles of wettability and surface tension in droplet formation during inkjet printing. Sci. Rep. **7**(1), 11841 (2017). https://doi.org/10.1038/s41598-017-12189-7